7-2009

The Effect of Negative-Energy Shells on the Schwarzschild Black Hole

Jeffrey Hazboun
Utah State University

Tevian Dray
Oregon State University

General Relativity and Gravitation manuscript No.
(will be inserted by the editor)

The Effect of Negative-Energy Shells on the Schwarzschild Black Hole

Jeffrey S Hazboun · Tevian Dray

3 July 2009

Abstract We construct Penrose diagrams for Schwarzschild spacetimes joined by massless shells of matter, in the process correcting minor flaws in the similar diagrams drawn by Dray and 't Hooft [1], and confirming their result that such shells generate a horizon shift. We then consider shells with negative energy density, showing that the horizon shift in this case allows for travel between the heretofore causally separated exterior regions of the Schwarzschild geometry. These drawing techniques are then used to investigate the properties of successive shells, joining multiple Schwarzschild regions. Again, the presence of negative-energy shells leads to a causal connection between the exterior regions, even in (some) cases with two successive shells of equal but opposite total energy.

1 Introduction

Penrose diagrams are commonly used to describe the global structure of spacetimes. The mathematically rigorous construction of these diagrams, first given by Penrose [2] and Carter [3], involves a careful look at the asymptotic behavior of spacetime, as is well summarized in [4]. Such conformal diagrams are well adapted for showing the global structure of spacetimes containing null shells, and many examples of such Penrose diagrams can be seen in [5]. Dray and 't Hooft presented similar diagrams in [1], which described how spherically symmetric shells of massless matter affect Schwarzschild spacetime.

Although Penrose diagrams have been proposed for more involved spacetime structures, such as the collapse of stars and the evaporation of black holes [6], these are often presented without rigorous mathematical construction. Here we will extend the work of Dray and 't Hooft by carefully drawing Penrose diagrams in one global set of coordinates. This will allow us a visual means of investigating the structure of these Schwarzschild spacetimes joined by shells, as is particularly well demonstrated by our investigations of shells with negative energy density and of successive shells.

Jeffrey S Hazboun
Department of Physics, Oregon State University, Corvallis, OR 97331. E-mail: Jeffrey.Hazboun@gmail.com

Tevian Dray
Department of Mathematics, Oregon State University, Corvallis, OR 97331.
E-mail: tevian@math.oregonstate.edu

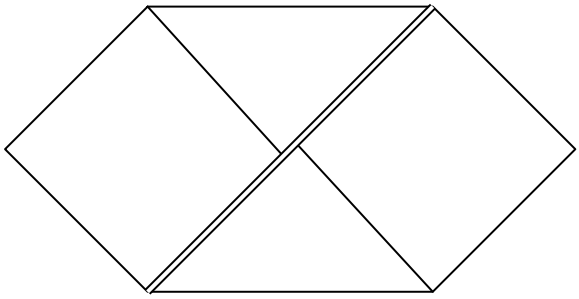

Fig. 1 The Penrose diagram of a particle crossing the horizon as drawn in [7] Here we see that the Dray-'t Hooft solution has a shift in the horizon as one crosses the world line of the shell (the double line). Note that requiring the outer boundary to be the same as for ordinary Schwarzschild, as drawn here, prevents the shifted horizon (the broken single line) from being drawn at 45°.

The paper is organized as follows. In Section 2 we present the Penrose diagrams given in [1], which we then redraw more accurately in Section 3. In Section 4, we consider the effect of shells with negative energy density, showing that such shells can be used to construct traversable wormholes. In Section 5, we consider the effect of successive, non-intersecting shells, paying particular attention to the case of concentric shells of equal but opposite total energy. Finally, in Section 6, we discuss our results.

2 Joined Schwarzschild Penrose Diagrams

Dray and 't Hooft [1] constructed solutions of the Einstein field equation which represent two separate Schwarzschild spacetimes joined along spherically symmetric shells of massless matter. These shells are described by stress-energy tensors of the form

$$T_{uu} = \frac{\kappa}{4\pi}\delta(u) \qquad m_1 = m_2 \tag{1}$$

$$T_{uu} = \frac{m_1(m_2 - m_1)}{\pi\alpha r^2}\delta(u-\alpha) \qquad m_1 \neq m_2 \tag{2}$$

where u is a null Kruskal-Szekeres coordinate, $u = 0$ corresponds to the horizon, and the shell is located at $u = \alpha$. One of the more interesting features of spacetimes joined in such a manner, first shown explicitly in [7] and drawn in Figure 1, is that there is a shift in the horizon as an observer crosses over the shell. This result is easily explained in the case where the shell separates two Schwarzschild regions with different masses, since $r = 2m_1$ and $r = 2m_2$ will meet the shell, on their respective sides, at different points. Surprisingly this shift also occurs in the case where both regions are of equal mass and the shell is at the horizon.

A careful look at the Penrose diagram in Figure 1 shows that it is impossible to draw both the shifted and unshifted horizons as null lines while preserving the boundary. The horizons are null lines, and should therefore be kept at 45° as we cross the boundary. The center picture in Figure 2 is therefore drawn incorrectly. The off-horizon, unequal-mass Penrose diagrams are correct, if we assume each region is drawn in its own set of coordinates, however, they are misleading as drawn. We will show below that drawing the entire diagram with one set of coordinates changes the shape of the singularity, which is the only line not

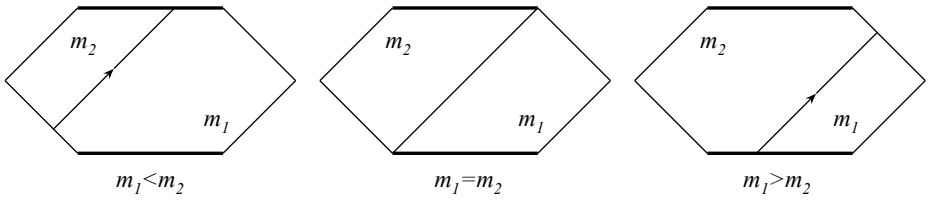

Fig. 2 Dray-'t Hooft Conformal Diagrams: These diagrams depict the three cases considered by Dray and 't Hooft for a single null shell [1]. The first diagram represents a shell of positive energy density symmetrically collapsing to the singularity. The center picture is a shell at the horizon, and the last diagram shows a shell expanding from the singularity out to infinity.

drawn along a null trajectory. By drawing the pictures, and especially the boundary, more accurately, it is possible to obtain physical information directly from the diagrams, such as the relative shift in horizons and the relative positions of horizons.

3 Shifted Diagrams

We begin by reviewing the construction of the spacetimes in [1]. In order to glean as much physical understanding from these Penrose diagrams as possible, we shall be pedantic about the use of one coordinate system to draw the entire spacetime. Throughout this paper, u_1 and v_1 will refer to the coordinates of the region where $u < \alpha$ and u_2 and v_2 will refer to the coordinates of the region where $u > \alpha$. We first assume that the coordinates in Region 2 can be expressed as functions of u_1 and v_1. As shown in [1], by requiring the metric to be continuous at the join we get two relations,

$$\frac{dv_2}{dv_1} = \frac{m_1^3}{u_2'(\alpha)m_2^3} e^{-\frac{r}{2m_1}+\frac{r}{2m_2}|_{u_1=\alpha}} \tag{3}$$

$$\frac{\alpha}{m_1} = \frac{u_2(\alpha)}{m_2 u_2'(\alpha)} \tag{4}$$

which can be used to find u_2 and v_2 as functions of u_1 and v_1, respectively. It is important to note that (3) in principle yields a global relationship between v_1 and v_2, whereas (4) refers to a boundary condition that applies only at the shell.

3.1 Equal Mass Diagrams

In the case of a shell at the horizon, (3) and (4) can be simplified extensively, resulting in the expressions

$$\begin{aligned} u_2 &= u_1 \\ v_2 &= v_1 + \kappa \end{aligned} \tag{5}$$

where κ is the constant from the T_{uu} component of the stress energy tensor in (2). We have also assumed the relationship in (4) is a global relationship, and linear in u_1. Penrose diagrams are traditionally drawn using the canonical asymptotic transformation

$$U = \arctan(u), \quad V = \arctan(v) \tag{6}$$

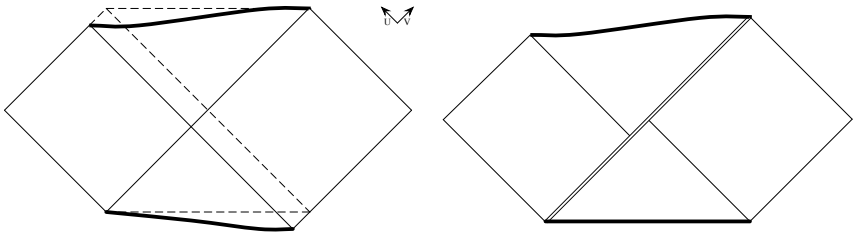

Fig. 3 Equal Mass Diagrams: The first diagram in this figure is the Penrose diagram drawn for a spacetime with coordinates u_2 and v_2 as in equations (5). The bold lines are the singularities drawn in the shifted coordinates. The second figure represents the Dray-'t Hooft spacetime with the shell represented by the double line at the horizon.

By making the substitutions from (5) before doing the asymptotic coordinate transformation on the spacetime, so that

$$U = \arctan(u_2), \quad V = \arctan(v_1 + \kappa) \tag{7}$$

we obtain a Penrose diagram that differs from the standard "straight" Schwarzschild conformal diagram.

The first diagram in Figure 3 shows the shifted coordinate system drawn on top of the straight Penrose diagram for Schwarzschild spacetime; both superimposed diagrams represent a Schwarzschild spacetime of the same mass. The most striking change in the diagram is in the shape of the singularities, which are no longer perfectly horizontal. In the second diagram in Figure 3, we have split the spacetime along the location of the shell, at the horizon, and joined it to a region with unshifted coordinates. This accurately depicts the entire Dray-'t Hooft spacetime, drawn in the coordinates of the unshifted region.

The set of coordinates the diagrams are drawn in is of course arbitrary; we could just as easily have drawn these pictures using the u_2 and v_2 coordinates. This would have the effect of curving the white hole singularity instead of the black hole singularity, but the relative shift in the horizon would be the same.

3.2 Unequal Mass Diagrams

The case of a shell that is not at the horizon is more complicated than the equal mass (at the horizon) case. Going back to the general relations (3) and (4) and solving for the Region 2 coordinates as functions of the Region 1 coordinates, we get

$$u_2 = u_1 + \alpha\left(\frac{m_2}{m_1} - 1\right) \tag{8}$$

$$v_2(v_1) = \left(m_1 \mathscr{W}\left(-\frac{v_1\alpha}{e}\right) + 2(m_1 - m_2)\right) \frac{m_1}{\alpha m_2^2 u_2'(\alpha)} e^{\frac{m_1}{m_2}\left(\mathscr{W}\left(-\frac{v_1\alpha}{e}\right)\right)} \tag{9}$$

where $\mathscr{W}$ is the Lambert W function (also known as the Product Log), [8]. The integration constant, found by setting $v_2(v_1) = v_1$ at the singularity, is identically zero. There is a freedom in the choice of $u_2(u_1)$, and we have chosen a simple linear relationship that satisfies (4). Also, (8) again implicitly assumes that the relation in (4) is true for all values of u_1. These functions are then used to draw the Penrose diagram in Region 2. The singularity in Region 2, where $u_2 v_2 = 1$, is computed as the nested function $u_1(u_2(v_2(v_1)))$. The

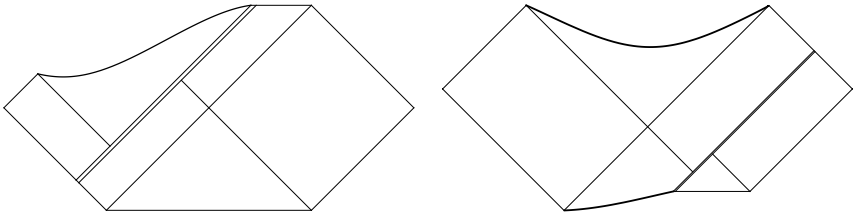

Fig. 4 Unequal Mass Diagrams: On the left is the diagram for a spacetime with a shell at $\alpha = \frac{1}{2}$, and $m_2 = \frac{5}{4}m_1$. On the right is a diagram for the case where $\alpha = -\frac{3}{2}$, and $m_2 = \frac{4}{5}m_1$

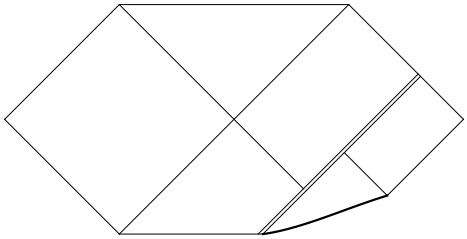

Fig. 5 Negative α diagram drawn in u_2, v_2 coordinates: Here we have drawn the entire diagram in the Region 2 coordinates. By using these coordinates, there is no need to use an arbitrary function.

shifted horizon is drawn as a null line starting at $r = 2m_2$ on the shell. Figure 4 shows the shifted diagrams for shells with positive energy density that are collapsing or expanding, respectively.

The second diagram in Figure 4, with $\alpha < 0$, results in a shifted white hole singularity. This singularity, however, does not lie within the light cone of the shell, and cannot therefore be described by the metric continuity equations, (3) and (4), that we have previously used to construct the shifted coordinates. In Figure 4, we have chosen a linear relationship for $v_2(v_1)$. In fact, the Lambert W function becomes complex at $\frac{1}{\alpha}$, mathematically dictating that the original coordinate relationship (9) is no longer useful. The choice of coordinate extension used is completely arbitrary, so long as modest continuity conditions hold. We can nonetheless use the relationships in (8) to fully describe this case if we instead treat the u_1 and v_1 coordinates as functions of u_2 and v_2. Figure 5 shows a Penrose diagram for a shell with $\alpha < 0$, with the Region 1 singularity drawn in u_2 and v_2 coordinates. Similar comments apply to the case $\alpha > 0$, with the roles of the regions reversed.

These diagrams reveal some important characteristics of these spacetimes. As shown in Figure 4, when a shell passes over an observer, their relative position with respect to the horizon transverse to the shell is changed. In the positive α case (the first diagram in Figure 4), an observer in the (left) asymptotic region may even be shifted into the black hole.

For completeness, we apply similar techniques to the next case considered in [1] and look at the Penrose diagrams when $m_1 = 0$ or $m_2 = 0$. Here we use a shell with a trajectory along the null Kruskal-Szekeres u-direction, in order to retain the standard orientation of the Penrose diagram for Minkowski space. Again we see that the singularities are no longer straight, as shown in Figure 6.

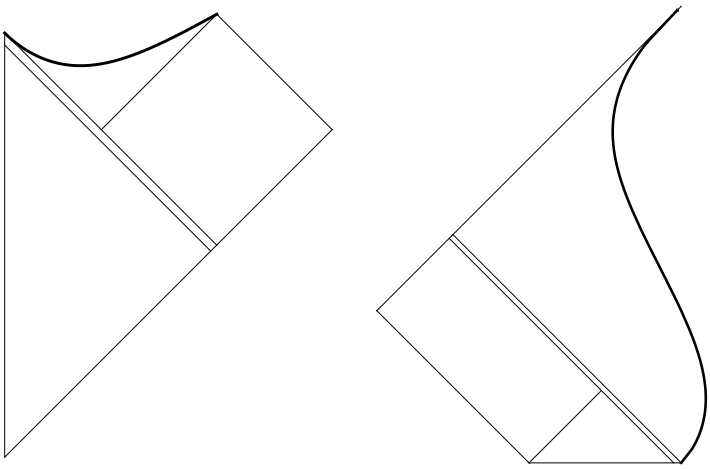

Fig. 6 Minkowski↔Schwarzschild Mass Diagrams: On the left is the diagram for a spacetime with a shell at $\alpha = \frac{1}{2}$. On the right is a diagram for the case where $\alpha = -1$.

In constructing Figure 6, we have again used a linear function to describe the relationship between the coordinates transverse to the shell, which are now v_1 and v_2. In the second diagram, the simplest linear relationship that satisfies (4) is

$$v_2 = \frac{2m_1 v_1}{\alpha} \tag{10}$$

Note that the second diagram in Figure 6 is not changed when the mass of Region 1 is changed.

4 Negative Energy Shells and Wormholes

Until this point, we have been careful to consider only spacetimes containing shells with positive energy density. Using our techniques, however, it is elementary to study the effects of shells with negative energy density. Looking explicitly at the energy density component of the stress-energy tensor, transformed to the canonical Schwarzschild coordinates,

$$-T_t{}^t = \frac{(m_2 - m_1)}{4\pi r^2} \frac{|\alpha|}{\alpha} \delta(r - r_0) \tag{11}$$

we see that the sign of the energy density depends on both the sign of the change in mass between the two regions and on the sign of α. This differs from the similar expression given in [9], where the dependence on α has been omitted, since negative energy density shells were not being considered. The dependence on α arises because the sign of α dictates whether the shell is expanding or contracting. Note that we have not concerned ourselves with the "how" of negative energy density, but only its effects. For detailed discussions of negative energy in general relativity, see Ford and Roman [10].

When we draw diagrams with negative energy density shells, there are some important changes in the structure of the spacetime that are easily seen by looking at our Penrose diagrams. In Figure 7, we see that the horizons, in both cases, have shifted in the positive

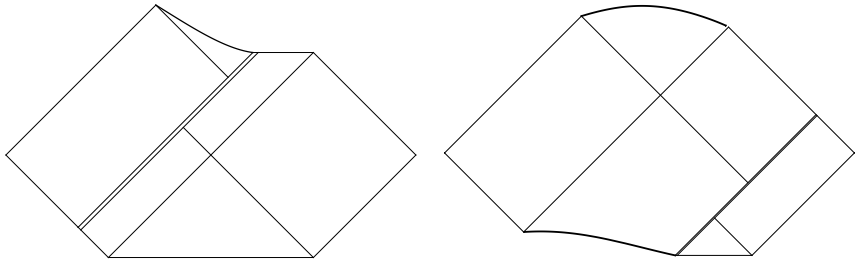

Fig. 7 Unequal Mass Diagrams with Negative Energy Density Shells: The first diagram is for a spacetime with a shell at $\alpha = \frac{1}{2}$, and $m_2 = \frac{4}{5}m_1$. The second diagram depicts the case where $\alpha = -\frac{3}{2}$, and $m_2 = \frac{5}{4}m_1$. Note the shift has opened a gap between the two u_1 and u_2 horizons, that a time-like or light-like trajectory can pass through.

v direction. This shift in the horizon allows a null geodesic to pass through the Einstein-Rosen bridge to the other asymptotically flat region of the spacetime. These figures show this important attribute of the spacetime with little computational effort.

Wormholes in spherically symmetric spacetimes have been discussed at length by Morris and Thorne [11,12] and Visser [13,14]. Each of these authors demonstrates that the resulting spacetime must have a stress-energy tensor that compromises either the weak energy condition or the averaged weak energy condition. It is therefore not surprising that our simple wormholes require negative energy density for their construction.

5 Successive Shells

Our techniques can be easily generalized to draw Penrose diagrams of spacetimes with multiple Schwarzschild regions joined along successive shells. Through most of this paper, and in particular in Figures 4 and 7, we have used the u_1, v_1 coordinates to draw the joined Penrose diagrams. In Figure 5 we drew Penrose diagrams using the u_2, v_2 coordinates. It is straightforward to combine two such diagrams, resulting in a spacetime that contains two successive shells, drawn using the coordinates from the middle region. These spacetimes satisfy the boundary conditions in [1] at each shell, but the diagrams can be obtained by combining the appropriate "jigsaw puzzle pieces" from Figures 4 and 5.

For example, in Figure 8 we have drawn two diagrams, each with two shells. The first diagram shows a spacetime with three Schwarzschild regions, joined by two shells with positive energy density, while the second diagram represents three Schwarzschild regions joined by two shells of negative energy density.

The same Penrose diagrams can also be drawn using the Region 1 coordinates. In this case Region 3 is drawn by first relating the coordinates in Region 3 to those in Region 2 using (3) and (4), and then inserting the known functional dependence of the Region 2 coordinates on the Region 1 coordinates, obtaining expressions of the form $u_3 = u_3(u_2(u_1))$ and $v_3 = v_3(v_2(v_1))$. While difficult to evaluate by hand, *Mathematica* has no difficulty working with these composite functions, leading to diagrams such as those shown in Figure 9, drawn entirely using the Region 1 coordinates.

It is particularly interesting to consider concentric shells with equal but opposite total energy. Looking at Figure 10, it is obvious that there is a net shift in the horizons, even though the Region 1 and Region 3 Schwarzschild regions have the same mass. This net shift

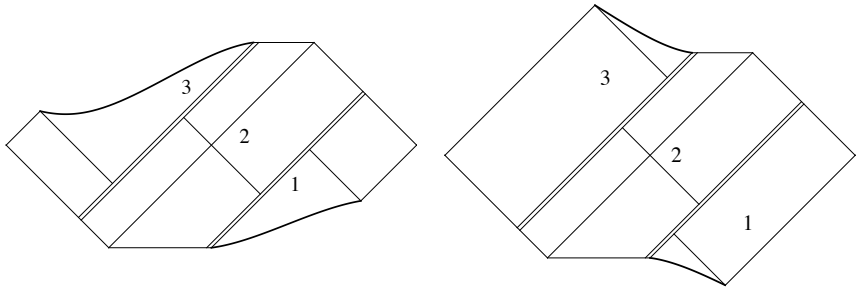

Fig. 8 Two Successive Shells, Drawn in u_2 and v_2 coordinates: Here the first diagram has two shells of positive energy density, while the second diagram has two shells of negative energy density.

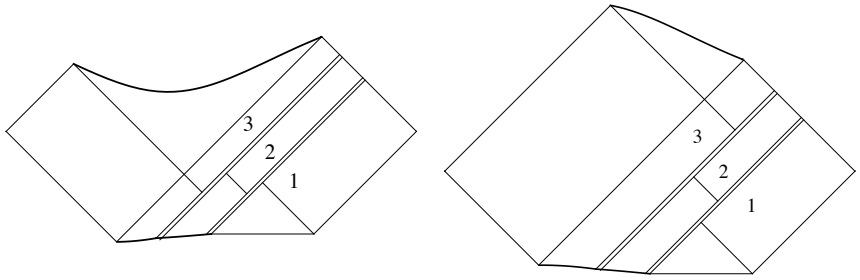

Fig. 9 Two Successive Shells, Drawn in u_1 and v_1 coordinates: The first diagram has two shells of positive energy density, while the second has two shells of negative energy density

arises because each shift is dependent on the energy density, not the total energy, as can also be seen from the dependence of the stress-energy tensor on the radius of the shell in (11). Since the inner shell will always be smaller, and hence more dense, than the outer shell, there will always be a net shift when the shells have equal but opposite total energy.

6 Discussion

The primary purpose of this work has been to outline a method for drawing accurate Penrose diagrams for Schwarzschild-like spacetimes containing spherical shells of massless matter. This method is straightforward: solve the boundary conditions given in [1], then construct particular diagrams numerically. This construction was originally motivated by the observation that the diagrams given in [1] cannot in fact be accurate, as discussed in Section 2. However, the accurate diagrams constructed in Section 3 do not in fact contain any new physical insight; one could argue that the diagrams in [1] are indeed correct, even though some artistic liberty was taken.

The situation is different when negative energy shells are considered. First of all, as discussed in Section 4, even a single negative energy shell leads to traversable wormholes; the shift goes "the other way". Of even greater interest, we showed in Section 5 that nested shells of equal but opposite total energy still lead to traversable wormholes — provided the negative energy shell is inside the positive energy shell. Thus, should "nested" positive/negative-energy particle pairs exist, they would generate traversable wormholes!

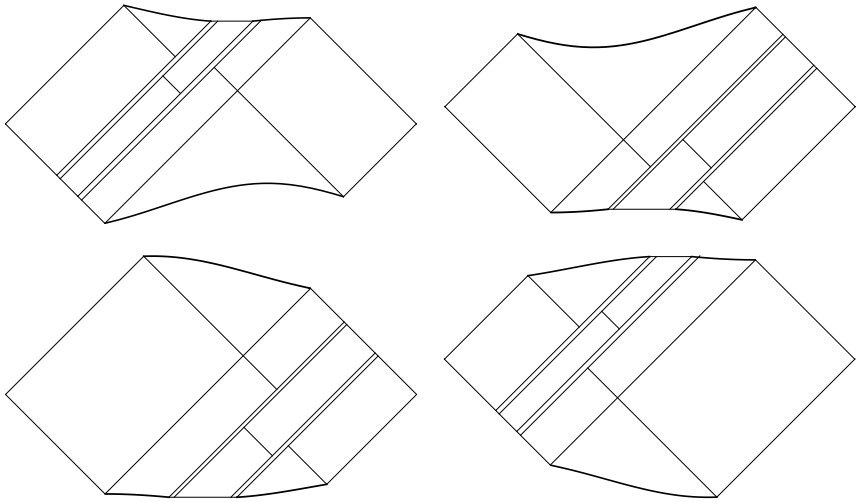

Fig. 10 Two Shells with Equal but Opposite Total Energy: These four figures cover the four possible configurations of two concentric shells with equal but opposite total energy, drawn in the u_2 and v_2 coordinates. The first two figures represent concentric shells, where the inner shell has positive energy density. The last two figures are Penrose diagrams of concentric shells where the inner shell has negative energy density, and the overall shift allows for travel between the exterior Schwarzschild regions.

How big would such a wormhole be? As a characteristic scale, we determine the "width" between the transverse horizons in Regions 1 and 3. As a measure of this width, we compute the difference Δt in Killing time between the null extensions of those horizons into Region 2, measured along a null line parallel to the shells. For definiteness, we consider the situation shown in the lower left diagram in Figure 10. In null Kruskal-Szekeres coordinates,

$$t = 2m_2 \log\left(-\frac{v_2}{u_2}\right) \tag{12}$$

Inserting $v_1 = 0$ (respectively, $v_3 = 0$) on the transverse horizon in Region 1 (respectively, Region 3) into (9), and then into (12), using (4), and subtracting, almost everything cancels (since we are assuming u is constant), and we are left with

$$\Delta t = 2m_2 \log\left(\frac{\alpha_1}{\alpha_2}\right) \tag{13}$$

Thus, the "width" of the wormhole depends on the "distance" between the shells, as given by the ratio of the α_i, which can be chosen arbitrarily.

Remarkably, (13) depends on the background mass $M = m_1 = m_3$ only through the Schwarzschild mass of Region 2, which satisfies $m_2 = M - m$, where m is the (magnitude of the) total energy in each shell. If we assume that $m << M$, then Δt scales linearly with M. Even if we choose the α_i to be nearly the same, the effect might, in principle, be large enough to measure. For example, if $\frac{\alpha_1}{\alpha_2} = 1.01$, m is the electron mass, and M the mass of the sun, then $\Delta t \approx 29$ m $\approx 10^{-7}$ s.

In summary, we have succeeded in constructing "jigsaw puzzle pieces" which can be combined to analyze more complex arrangements of shells, such as the successive shells considered in Section 5. Although new pieces do need to be constructed to analyze scenarios

with additional shells, this method is still a useful tool for analyzing the effect of those shells. In future work, we hope to adapt these methods so as to be able to analyze intersecting shells, as were also considered by [1].

Acknowledgements This paper is an extension of the paper submitted by JSH in partial fulfillment of the degree requirements for his M.S. in Physics at Oregon State University [15].

References

1. Tevian Dray and Gerard 't Hooft, *The effect of spherical shells of matter on the Schwarzschild black hole*, Commun. Math. Phys. **99**, 613–625 (1985).
2. Roger Penrose, *Zero rest-mass fields including gravitation: Asymptotic behavior*, Proc. Roy. Soc. **A284**, 159–203 (1965).
3. B. Carter, *Complete Analytic Extension of the Symmetry Axis of Kerr's Solution of Einstein's Equations*, Phys. Rev. **141**, 1242 (1966).
4. Robert Geroch, *Asymptotic structure of space-time*, in: F. Paul Esposito and Louis Witten, editors, **Asymptotic Structure of Space-Time**, Plenum Press, New York and London, 1977, pp. 1–105.
5. Claude Barrabés and Peter A. Hogan, **Singular Null Hypersurfaces in General Relativity: Light-Like signals from violent Astrophysical Events**, World Scientific, New Jersey, 2003.
6. Sean M. Carroll, **Spacetime and Geometry: An Introduction to General Relativity**, Addison and Wesley, San Fransisco, 2003.
7. Tevian Dray and Gerard 't Hooft, *The Gravitational Shock Wave of a Massless Particle*, Nucl. Phys. **B253**, 173–188 (1985).
8. R. M. Corless, G. H. Gonnet, D. E. G. Hare, D. J. Jeffrey and D. E. Knuth, *On The Lambertw Function*, Adv. Comput. Math. **5**, 329 (1996).
9. Tevian Dray and T. Padmanabhan, *Conserved quantities from piecewise Killing vectors*, Gen. Rel. Grav. **21**, 741–745 (1989).
10. Larry H. Ford and Thomas A. Roman, *Motion of inertial observers through negative energy*, Phys. Rev. **D48**, 776–782 (1993).
11. Michael S. Morris and Kip S. Thorne, *Wormholes in space-time and their use for interstellar travel: A tool for teaching general relativity*, Am. J. Phys. **56**, 395–412 (1988).
12. Michael S. Morris, Kip S. Thorne, and Ulvi Yurtsever, *Wormholes, Time Machines, and the Weak Energy Condition*, Phys. Rev. Lett. **61**, 1446–1449 (1988).
13. Matt Visser, *Traversable wormholes: Some simple examples*, Phys. Rev. **D39**, 3182–3184 (1989).
14. Matt Visser, *Traversable wormholes from surgically modified Schwarzschild space-times*, Nucl. Phys. **B328**, 203–212 (1989).
15. Jeffrey S. Hazboun, *The effects of negative-energy shells on schwarzschild geometry*, Master's thesis, Oregon State University (2008).